Advanced Modelling of Solar Energy Based Ice Storage Systems

Vivek J. Glasswala[1], Dr. Andy Gradel[1], Tushar Sharma[1], Dr. Daniel Carbonell[2], Prof. Dr. Tobias Plessing[1]

[1] Institute for Hydrogen and Energy Technology of Hochschule Hof, Hof (Germany)

[2] SPF Institute for Solar Technology, Rapperswil (Switzerland)

Abstract

Storage of fluctuating renewable energy sources is of elementary importance for decarbonizing the energy system. Ice storage systems can be used for this purpose in industrial cooling applications. For an accurate process design, an existing model was extended, improved in accuracy, and integrated into a complete system simulation. The simulation was used to numerically calculate the key performance indicators on all relevant processes of the storage tank, i.e. sensible cooling and heating, freezing and melting. The numerical model was validated with experimental results for a storage tank of 10 m^3 operating under real conditions using ice-on-coil heat exchangers coupled with the ground. The model predicted the ice fraction, heating capacity, average storage temperature as well as the output temperature of the heat transfer fluid with an accuracy above 98 % for the processes of melting and sensible heating.

Keywords: Ice Storage, Industrial Cooling, numerical modelling, TRNSYS simulation

1 Introduction

In order to reach a carbon neutral sustainable future, the energy supply system needs to be integrated with renewable resources. Apart from the residential cooling applications, sectors such as dairy, brewery, bakery, and food production also have a cooling demand with the temperature range from 0°C to 10°C. Using the renewable energy sources for such demands shows potential in cost and carbon emission reduction. However, fluctuating and unpredicted behavior of renewable alternatives such as solar or wind energy require energy storage systems. A promising solution to this challenge is the integration of thermal energy storage (TES) with the renewable resources. One example of such a system integration is the usage of an ice storage tank combined with a chiller. The chiller operated by electrical energy from a photovoltaics system can convert electrical energy into thermal energy, which can be used directly for the cooling demand or can be stored further into an ice storage. One of the advantages of such a system is the effective load shifting during the peak demand.

Since these systems are non trivial, a complete system simulation is necessary before designing a real system. There have been many studies conducted to check the performance of the ice storage with different heat exchanger geometries such as capillary mat (CM) and flat plate (FP) (Carbonell et al., 2017). In order to achieve an accurate process design, numerical models of such systems are available to forecast the effectiveness and energy saving potential. For this research process, a numerical model for ice storage namely Type 861 with the coiled heat exchanger geometry available in the TRNSYS has been considered. A complete system simulation was conducted to check the key performance indicators of an ice storage as well as to validate the model with the data collected from an experimental setup.

1.1 Ice Storage

Earlier in the history of the ice storage, industries such as breweries, dairies, and meat production with huge cooling requirement for product storage, collected and stored the ice from rivers during the winter season in so-called ice cellars, rather than using the machine made ice bars (Goeke, 2021). The modern version of ice cellars are figuratively ice storage tanks. The ice storage consists of heat exchanger, storage material, and the reservoir. Since the heat transfer occurs only between the surface of the heat exchanger and storage material,

10.18086/swc.2023.04.06 Available at http://proceedings.ises.org

most clever arrangement with the highest possible surface area is necessary. Some modern versions of the ice storages are shown in the Fig. 1.

Fig. 1: (a) Cylindrical Ice storage with helical coil heat exchanger geometry from Viessmann Werke (on left)
(b) Cuboidal Ice storage with U-type capillary mat heat exchanger from Clina (on right)

Ice storage technology is most widely applied example of latent thermal heat storage (LTES). The incorporation of LTES into practical application depends largely on the phase transformation capability of the thermal storage material. Due to the ability to undergo phase transformation under the isothermal conditions, the materials would freeze at constant temperature when cooled below the melting point. This unique phenomenon provides the storage material with the name *"Phase Changing Material (PCM)"*. Most significant object of latent heat storage is the possibility to store a large amount of energy within a small temperature range (Kalaisalvam and Parameshwaram, 2014).

The latent and sensible energy storage is explained (Kalaisalvam and Parameshwaram, 2014) by the mathematical description of the estimated enthalpy of fusion:

$$2.5RT_m < \Delta h_{m,mol} < 5RT_m \qquad \text{(eq. 1)}$$

Where T_m is the melting temperature, $h_{m,mol}$ is the molar heat of fusion, and R is the molar gas constant.

When the PCM is heated from the initial temperature T_1 to the melting temperature T_m and further to the temperature T_2, the heat stored in the material is:

$$Q_{Total} = Q_{sensible,solid} + Q_{latent} + Q_{sensible,fluid} \qquad \text{(eq. 2)}$$

$$Q_{Total} = m \cdot c_{p,\text{solid}}(T_m - T_1) + m \cdot \Delta h_m + m \cdot c_{p,\text{fluid}}(T_2 - T_m) \qquad \text{(eq. 3)}$$

Ice thermal energy storage systems (ITES) are used in many fields. For a regenerative-fed cooling application of above 0 °C, ice storage can be used as the low cost latent heat storage. The design parameters for ITES systems depend on a wide variety of variables, such as volume, mode of operation, type of heat exchanger, and loading and unloading characteristics for better performance during cooling demand. For an accurate process design, it is essential to have the simulation models as accurate as possible, because a wrong design can endanger the productivity of the respective industries or can consume more unnecessary fossil resources from the backup solutions. This research process targets the total simulation including modeling and validation of combined mathematical model available for ice storage (Type 861) described in Carbonell et al. (2018) with the ground model (Type 709) described in Carbonell et al. (2016) as boundary condition in TRNSYS using the real conditions and available data from the small experiment setup. The process includes the validation of melting and heating behavior of this particular mathematical model.

2 Research Process

In order to run a simulation, certain data are required to define various properties, boundary conditions and input fields. These environmental parameters allow us to observe and understand the effects of each parameter on the performance of the system. This helps to define the system more accurately in the simulation program and to identify the completeness of the mathematical model. These data can be obtained either from the manufacturers or from the sensors installed in the test rig. Data such as the dimensional characteristics of the component, maximum and minimum operating temperatures, maximum volume, etc. are available in the respective operating manuals. On the other hand, the real-time operating data are recorded during the test from the sensor measurements.

For the validation of the performance of the ice storage, a reference test bench for the heat pump with ice storage was considered. This has been designed and set up in the energy laboratory of the Münchberg campus of Hof University of Applied Sciences.

2.1 Test bench and experiment

The basis for this research process was laid in a previous research project, which aimed to design and construct two types of heat pump systems to research and develop the solution to the ever increasing energy demand (Kätzel, 2015). The energy concept shown in Fig. 2 was used to develop the solar heat pump system with ice storage in the laboratory. As shown in Fig. 1, ice storage with spiral heat exchanger by Viessmann consists of a tank with built-in heat exchanger and distributor, which is buried in the garden and usually filled with untreated tap water. Solar air absorbers installed on the roof supply the heat extracted from the ambient air and solar radiation to the tank.

Fig. 2 illustrates the experiment setup available in the lab consisting of an ice storage tank with two different heat exchangers for the extraction and regeneration purpose. The primary circuit is connected to a heat pump that extracts heat from the water in the ice storage via coils through the cooled brine. This is also known as the extraction heat exchanger. The secondary circuit, which connects the solar air absorber with the ice storage tank, is called the regeneration circuit as it transfers the heat collected by the solar air absorber to regenerate the cold energy stored in the form of ice.

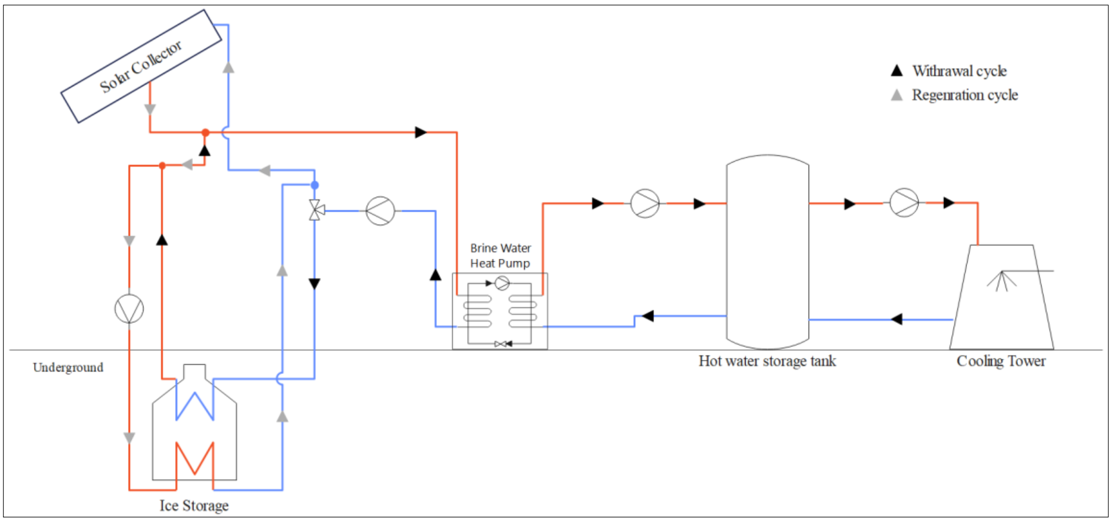

Fig. 2: Hydraulic schema of the test bench

The test bench consists of following main components:

- Brine/Water Heat Pump
- Ice Storage (Buried Underground)
- Solar Air Absorber
- Buffer Tank (Heating Circuit)
- Buffer Tank (Process Water)
- Control System

Depending on the active heat exchanger, all four processes mentioned above can be divided into the following two circuits:

- *Extraction/Withdrawal process*: During the withdrawal process, the heat energy is extracted from the PCM, resulting in cooling and eventually freezing of the PCM. Cooling and Icing/Freezing cycle – Highlighted by black arrows in Fig. 2.

- *Regeneration process*: During the regeneration process, the heat energy is released to the PCM, causing the PCM to melt and eventually heat up. Melting and Heating cycle – Highlighted by grey arrows in Fig. 2.

The challenge of this research process is to test the heating and cooling performance of the ice storage tank with coil heat exchanger. From various literature studies, there were few findings on the validation of ice storage with coil heat exchanger. In terms of a broader perspective, the Type 861 model was validated with capillary mats heat exchangers (Carbonell et al., 2018) and flat plates (Carbonell et al., 2017) and a similar model was validated with one year of monitoring data coupled with the ground using a de-icing ice storage concept (Carbonell et. al, 2016). However, the model lacked validation for ice-on-coil heat exchangers typically used in commercial applications. This validation process will lay base for more accurate predictions for component sizing according to the cooling and heating load profile of an industry.

The continuous experiment was conducted during summertime from *May 30, 2022 to June 18, 2022*. Sensor data were collected at minute intervals and converted into a *CSV* file format. Furthermore, the UA values are responsible for limiting the maximum power input and output to as well as from the water. Since all the phase occurring in the ice storage have different physical dynamics, the complete testing process is divided into four sequences namely,

- Cooling
- Freezing
- Melting
- Heating

Data recorded for each minute of total 20-day experiment helps to increase the accuracy of the validation and provides continuous data without interruption. In order to prepare the data for simulation input files and to simplify the display and behavior of the ice reservoir, the recorded data were also divided into four separate sequences described above.

When validating an ice storage system, the heat exchange rate between the heat exchanger and the PCM as well as the behavior of the PCM in the container are decisive factors. The heat transfer via the heat exchanger can theoretically be calculated by the mass flow through the extraction or regeneration heat exchanger and the temperature difference at the inlet and outlet of the corresponding heat exchanger coil as shown in equation 4.

$$\dot{Q} = \dot{m}C_p\left(T_{brine,out} - T_{brine,in}\right) \qquad \text{(eq. 4)}$$

The calculation of the ice fraction in the ice storage is performed with help of ultrasonic sensor. The ultrasonic sensor provides signals in mA, which is then converted into distance during the calibration process. Calibration was performed in the lab by fixing the ultrasonic sensor in still position and moving a flat plate in the reciprocating action to record the change in sensor value depending upon the distance between sensor tip and the flat plate.

After the calibration of the ultrasonic sensor, the ice fraction is calculated through following equation:

$$M_{fr} = \frac{A_{storage} \cdot \rho_{ice} \cdot \rho_w}{\rho_{ice} - \rho_w} \cdot \frac{(G_n - G_0)}{M_0} \cdot 100 \qquad \text{(eq. 6)}$$

Here, G_0 is the distance calculated from the initial signal from the ultrasonic sensor and G_n is given by:

$$G_n = \frac{U_n - b}{m \cdot 100} \qquad \text{(eq. 7)}$$

Where U being the sensor signal in mA.

2.2 Simulation

As mentioned above, the sensor data collected from different positions of the experiment test bench are utilized in the TRNSYS energy simulation software to create the most accurate digital test bench environment possible and to compare the simulation results with real measured values. A similar type of approach was performed in a previous study at the institute comparing two different heat exchanger geometries namely capillary mat and flat plate (Sharma et al., 2020).

One of the advancements during the research process was the correction of Nusselt number calculation in order to increase the accuracy of heat transfer in the numerical model of the coiled heat exchanger. The new implemented Nusselt number calculation is:

$$Nu = 8.14 * \left(1.98 + \frac{1.8 * D_h}{2 * r_{avg.coil}}\right) \quad \text{(eq. 8)}$$

Where, D_h is the hydraulic diameter of the heat exchanger pipe and $r_{avg.coil}$ is the average radius of the unevenly distributed coil geometry of the heat exchanger. All the required dimensional parameter of ice storage as well as of the heat exchanger is defined in the simulation as an input. Certain number of control volumes are also defined for the water on the ice storage in order to consider the thermal conduction between the water layers and the thermal stratification due to the water density gradient at different temperature. Before conducting an experiment, the initial storage temperature from two temperature sensors submerged in the ice storage at 1.5 m and 2.5 m was recorded to provide an initial condition to the simulation. For the context of this research, the ice storage is buried in the ground, which represents the system boundary.

Type 861 stands for the mathematical model of the ice storage and Type 709 for the boundary conditions of the storage buried in the ground, which have to be defined in the simulation. As in reality, both components are interconnected, thus the heat transfer between the concrete wall of ice storage and the soil as well as between the atmosphere and the soil should also take place in the simulation. Because of this coupling, the temperature of the soil in different layers will vary.

Fig. 3 shows the geometry and location values of the ice storage buried underground with the necessary sensors to collect the ground temperature as well as the storage temperature data.

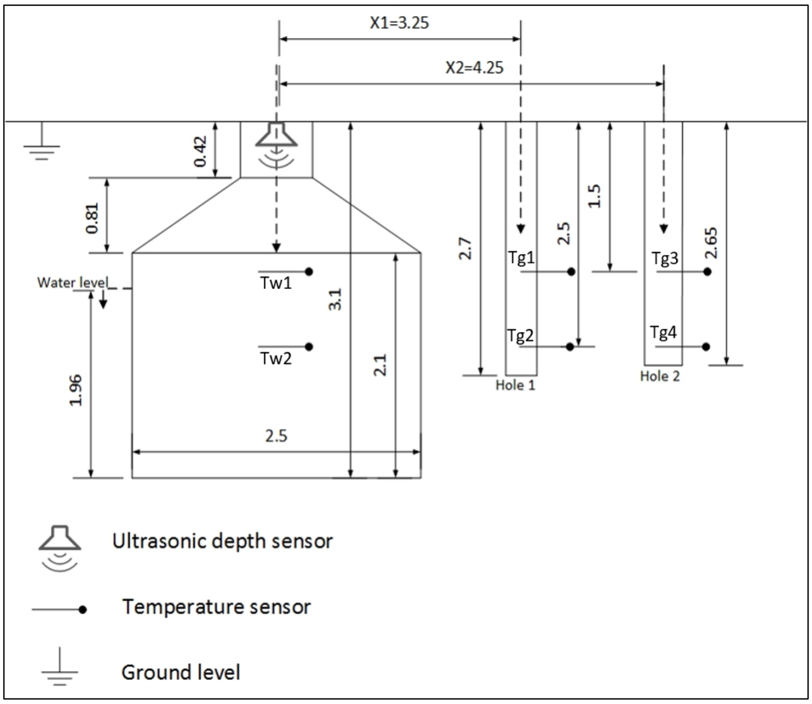

Fig. 3: Dimensional properties and sensor positions of the ice storage buried underground

The coupling between Type 861 and Type 709 was performed using the case study conducted by Carbonell et al., (2016). Considering Fig. 3, the total ground zone has the width of 4.90 m in X-direction and the depth of 5.63 m in negative Y-direction from the top left corner for this particular case. X-direction indicates the horizontal area taken into the consideration from the middle of the ice storage, where ultrasonic sensor has been installed, whereas negative Y-direction indicates depth and thus the vertical values from the ultrasonic sensor in respect to depth. The physical ground surface is then divided into 3-zones and 7-zones in X and in negative Y-direction respectively based on the property of the material. Zones in the X-direction consist PCM, concrete wall of the ice storage, and ground. Whereas as zones in the negative Y-direction consist PCM, concrete wall of the ice storage, and different beddings materials of the ground on which the reservoir foundation has been laid. Type 709 requires the initial ground temperature data at different depth of the ground.

However, as shown in Fig. 3, there are only four ground temperature sensors "*TgX* " available at 1.5 m and 2.5 m depth at 3.25 m and 4.25 m in X-direction respectively in the test bench. In order to provide more continuous temperature data of ground at different nodal points and control volumes, a depth dependent simple harmonic function was derived.

The soil temperature vary according to the different soil parameters and water content of the soil. From the study in Droulia et al. (2018) and in Máraquez et al. (2016), a depth and time dependent ground temperature behavior was derived and fitted using following approximate equation as a function of time:

$$T_{soil}(z,t) = T_m - T_p e^{-z\sqrt{\frac{\omega}{2\alpha}}} cos\left(\omega t - \varphi - z\sqrt{\frac{\omega}{2\alpha}}\right) \qquad \text{(eq. 9)}$$

Where,

T_m= Annual average temperature of soil in the stable layer (°C)

T_p = Amplitude (°C); the peak deviation of the function from zero. In this case the annual amplitude of the monthly average temperature cycle in the place

t = Time coordinate (s). Starting time is set to zero (t=0), meaning it begins from 1 January at 0 s. In special case where the average temperature of the ground of particular month is required, Simulation start time and end time can be set in the Matlab or Scilab model.

ω = Angular frequency (rad s^{-1}); $\omega = 2\pi/T$ is the period of sinusoidal. In this case annual temperature cycle $T = 365 * 3600 * 24$ s

φ = Phase (rad). When φ is non-zero, the entire waveform appears to be shifted in time by the amount φ/ω seconds. A negative value represents a delay, and a positive value represents an advance.

z = The depth in ground (m)

α = The ground thermal diffusivity (m s^{-2}) given by:

$$\alpha = \frac{k}{\rho C} \qquad \text{(eq. 10)}$$

ρ = Average soil density (kg m^{-3})

C = Specific heat capacity of soil (J kg^{-1} K^{-1})

k = Thermal conductivity of soil (W m^{-1} K^{-1})

Based on the equation, the mean temperature T_m and the amplitude of the surface temperature T_p were used as fitting parameters, which were in the acceptance range as can be seen in Table 1. The aim was to keep the difference between the measured value with sensor and the calculated value with equation 9 of the soil temperature as small as possible.

Tab. 1: Temperature measurements from the ground sensor and from ground-temperature estimation model

Process and Day	Sensors	Z – Depth m	T_{sensor} °C	$T_{g,Estimated}$ °C
Melting (Active Melting) 166th	T0	0	19.50	19.69
	TG1	1.5	13.10	13.57
	TG2	2.5	10.72	11.23
	TG3	1.5	13.57	13.57
	TG4	2.5	11.29	11.23
Heating (Active Heating) 169th	T0	0	19.01	19.96
	TG1	1.5	13.75	13.84
	TG2	2.5	11.00	11.45
	TG3	1.5	14.27	13.84
	TG4	2.5	11.42	11.45

Fig. 4 shows the graphical representation of the comparison between the measured temperature data from the sensors on the 166th day of the year and the calculated data from the Ground-Temperature-Estimation model on that particular day. The results obtained from the calculation were utilized to create the initial file, which was then specified as the initial boundary condition of the soil.

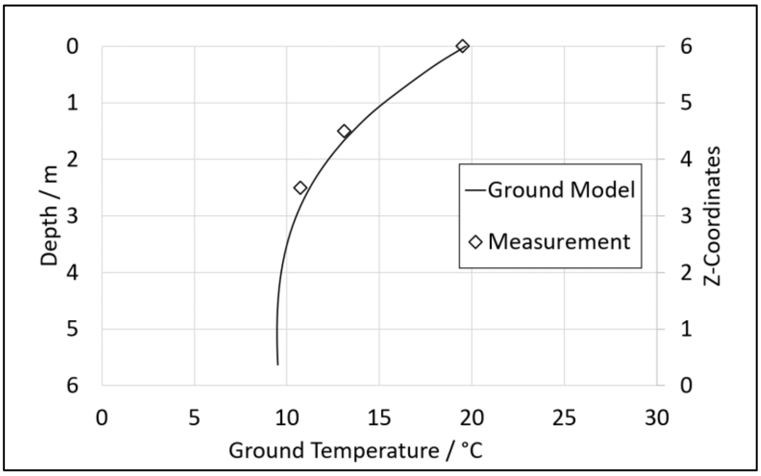

Fig. 4: Illustration of the comparison between the measured temperature data from the sensors and ground-temperature estimation model

From the hydraulics shown in Fig. 2, a simulation model is established using the following components in the TRNSYS:

Tab. 2 Essential component list for simulation model building in TRNSYS

Type	Description	Name
-	Equations and Constants	Equation Block
9	Generic Data Files – Skip Lines to Start – Free Format	Type 9c
25	Printer – No units printed to output file	Type 25f
46	Printegrator – Formatted – Monthly Periods	Type 46f
709	Ground Model	Type 709
861	Ice Storage model with ice-on heat exchangers	Type 861

3 Results and Validation

Once the boundary conditions for each critical component were established, the simulation was performed for melting and heating cycle. The printed file containing the simulation results was then prepared and plotted in Excel for better visualization.

3.1 Melting and Heating:

Once the ice percentage in the ice storage was reached at 80%, melting and heating of PCM was carried out. Melting in this case is considered until the mass of ice is zero and leads to the sensible heating of the PCM. As to be seen in the Fig. 5, the heating capacity follows the negative trend for this research process. The cooling capacity is referred as the positive value since the sole purpose of the ice storage is to deliver the cooling power. The sinusoidal behavior of the *Heating Capacity* as well as of the *Brine Outlet Temperature* as to be seen in the Fig. 5 and Fig. 6 respectively is due to the dependency of regeneration cycle on the solar absorber. Due to the available solar radiation during the daytime, the temperature level in the regeneration heat exchanger reaches its maximum. However, during the nighttime a sudden drop has been observed in the average temperature of the storage and only in the experiment during the melting cycle. It is because the Type 861 is not programmed to record the below zero value of the temperature of the PCM. During the melting cycle, ice on heat exchanger will first start to melt which then slowly transfer the heat from one layer of ice to another. Since there is no external heating energy available from the sun in the nighttime, the PCM far away from the heat exchanger wall still has the lower temperature values compared to the PCM closer to the wall. Due to this, there is a heat exchange in the PCM layers in all direction to reach the thermal equilibrium in the ice storage.

As the Type 861 does not record the below zero temperature value of the PCM, it does not show this behavior in the simulation. However, once that limitation is over, the model also follows the same behavior during the heating cycle as to be seen in Fig. 5. It also shows that the heating capacity of the ice storage in the experiment is similar to the results from the simulation conducted during melting and heating process. Considering the 0.50 °C average storage temperature as the beginning of heating, it begins roughly after 410th relative hour of the simulation. However, in the experiment, it begins quite early. It is because there are only two temperature sensors submerged in the PCM to record the temperature values and to calculate the average temperature of ice storage. They are installed near the heat exchanger wall, which affects the accuracy.

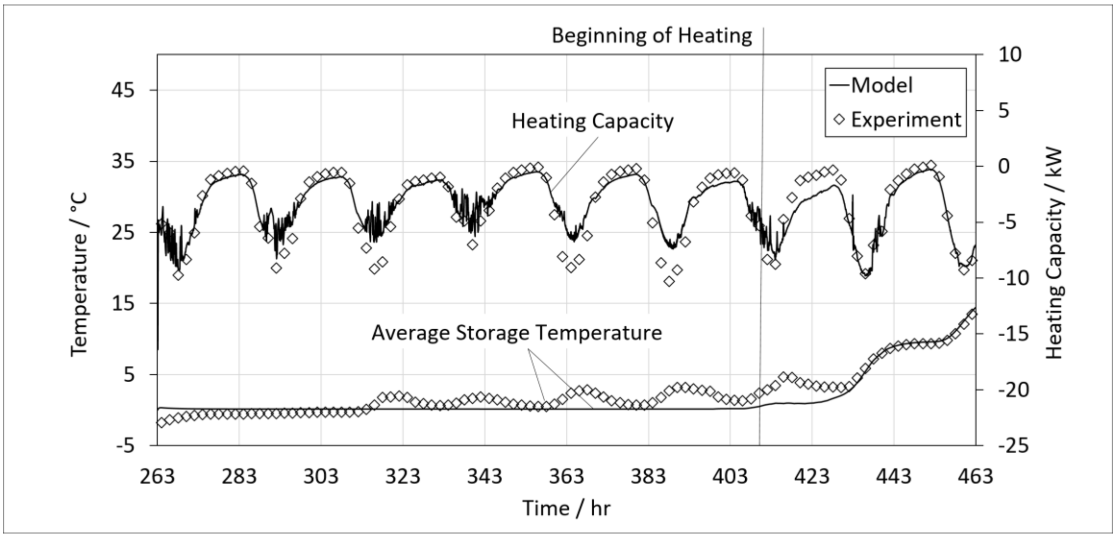

Fig. 5: Comparison of heating capacity and average storage temperature of ice storage during melting and heating process

In addition, there were no major discrepancies between the temperature estimated from the ground model and the data collected from sensors as shown in Fig. 6. As shown in Fig. 7, the initial ice fraction was defined at the 80% in the simulation to match the exact condition in the ice storage respective to storage temperature and the ice percentage calculated in from the ultrasonic sensor data available from the experiment.

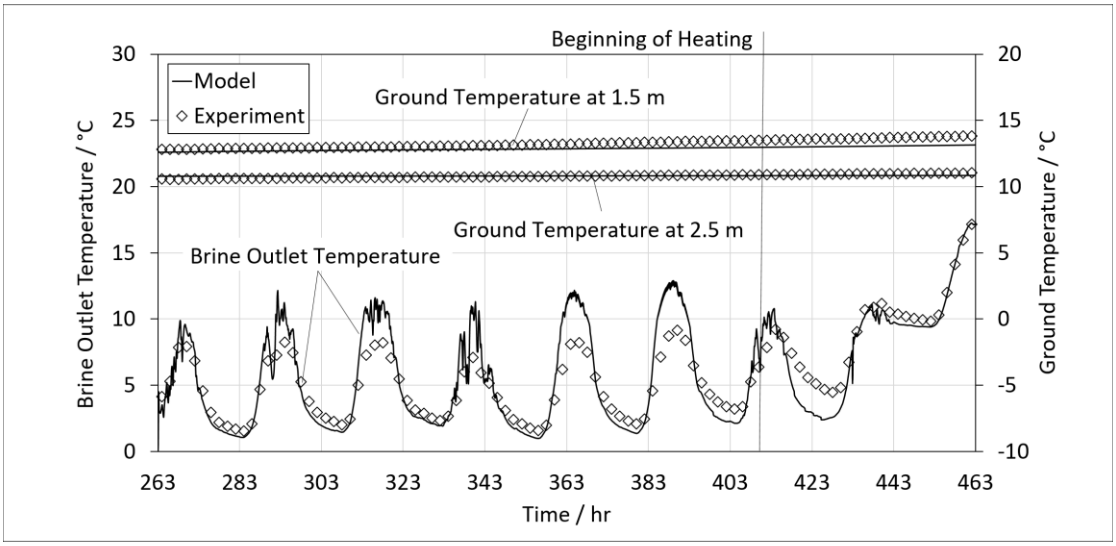

Fig. 6: Comparison of brine outlet temperature of ice storage and ground temperature during melting and heating process

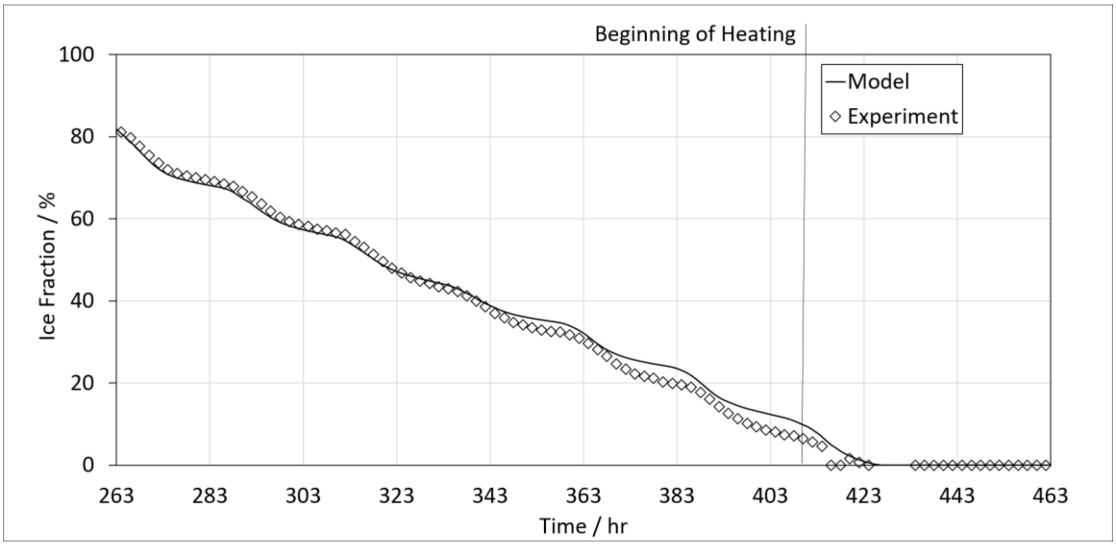

Fig. 7: Comparison of ice fraction in ice storage during the melting and heating process

4 Discussion

Using the standard root mean square average method for both experiment and simulation, the accuracy of each behavior is defined. The result data shows almost 99 % accuracy in ice fraction prediction following by 97 % accuracy in estimating the ground temperature from the recorded data. On an average, the heating capacity shows 86 % accuracy whereas brine outlet temperature and the average storage temperature achieves 94 % accuracy averagely during the whole sequence.

5 Acknowledgement

We thank the Hans Viessmann Technologie Stiftung and the Viessmann Climate Solutions SE for the financial support and we thank the Bavarian State Ministry for Science and Arts for the financial support under the project *KaWaTech*. We also thank the European regional development funds [EFRE] for financial support under the project *Grüne Technologie Werkstatt [GTW]* in cooperation with Genes Kältetechnik GmbH.

6 Reference

Carbonell, D., Philippen, D., Haller, M., Brunold S., 2016. Modeling of an ice storage buried in Modeling of an ice storage buried in the ground for solar heating applications - Validations with one year of monitored data from a pilot plant. Solar Energy: Journal of the international solar energy society 125, 398-414. https://doi.org/10.1016/j.solener.2015.12.009

Carbonell, D., Battaglia, M., Phillipen, D., Haller, M., 2017. Ice-Ex: Heat exchanger analysis for ice storage in solar and heat pump applications. Final report by Institute für Solartechnik SPF. https://doi.org/10.5281/zenodo.5596601

Carbonell, D., Battaglia, M., Phillipen, D., Haller, M., 2018. Numerical and experimental evaluation office storages with ice on capillary mat heat exchanger for solar-ice systems. International Journal of Refrigeration 88, 383-401. https://doi.org/10.1016/j.ijrefrig.2018.02.007

Droulia, F., Lykoudis, S., Tsiros, I., Alvertos, N., Akylas, E., Garofalakis, I., 2008. Ground temperature estimation using simplified analytical and semi-empirical approaches. Solar Energy 83, 211-219. https://doi.org/10.1016/j.solener.2008.07.013

Goeke, J., 2021. Thermische Energiespeicher in der Gebäudetechnik: Sensible Speicher, Latente Speicher, Systemintegration. Springer Nature, Germany. https://doi.org/10.1007/978-3-658-34510-5

Kalaisevam, S., Parameshwaram, R., 2014. Thermal Energy Storage Technologies and Sustainability. Elsevier Inc., London.

Kätzel, A., 2015. Masterarbeit: Planung und Aufbau eines Wärmepumpen-Prüfstandes mit einem Eisspeicher als Primärquelle. Hochscule Hof, Hof Germany.

Máraquez, J.M.A., Bohórquez, M.À.M., Melgar, S.G., 2016. Ground Thermal Diffusivity Calculation by Direct Soil Temperature Measurement – Application to very Low Enthalpy Geothermal Energy Systems. Sensors (Basel) 16(3), 306. https://doi.org/10.3390/s16030306

Sharma, T., Prof. Dr. rer. Honke, R., and Prof. Dr.-Ing. Plessing, T., 2020. Comparison of system performance of different types of Ice-battery for cooling application in industries. TFRE2020: International Conference on Recent Trends in Development of Thermo-fluid and Renewable Energy, NIT Arunachal Pradesh, India, 26-28 November. https://doi.org/10.1007/978-981-16-3497-0_46